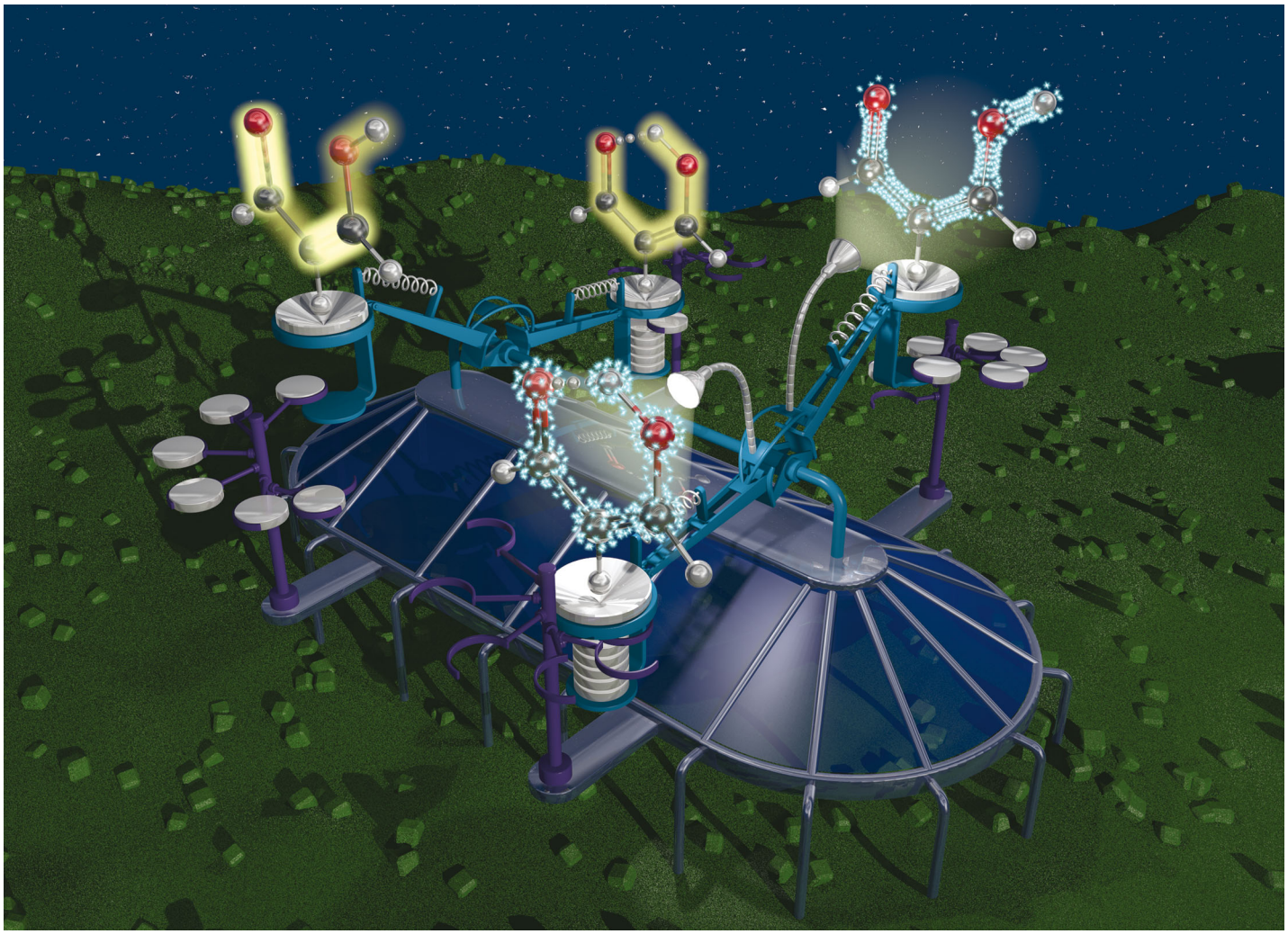

Showcasing the work at the Departments of Physical Chemistry at the Institute of Chemistry/UNAM and the University of Oviedo

Title: The nature of resonance-assisted hydrogen bonds: a quantum chemical topology perspective

This work addresses the nature of Resonance Assisted Hydrogen Bonds (RAHBs) by considering malonaldehyde whose H-bonded (closed) and non H-bonded (open) conformations are represented in the bottom and top of the seesaws respectively. Although delocalization indices are more uniform in the closed form (seesaw in the left), the number of delocalized electrons diminish on RAHB formation. The interaction is characterized by an increase/decrease in the intra-atomic/inter-atomic exchange energies as schematized with sparks in the highlighted seesaw in the right. The artwork is due to Mr Víctor Duarte Alaniz.

As featured in:

See Tomás Rocha-Rinza *et al.*, *Phys. Chem. Chem. Phys.*, 2016, **18**, 26383.

ROYAL SOCIETY OF CHEMISTRY

www.rsc.org/pccp

Registered charity number: 207890

PCCP

PAPER

View Article Online
View Journal | View Issue

Cite this: *Phys. Chem. Chem. Phys.*, 2016, **18**, 26383

The nature of resonance-assisted hydrogen bonds: a quantum chemical topology perspective†

José Manuel Guevara-Vela,[a] Eduardo Romero-Montalvo,[b] Aurora Costales,[a] Ángel Martín Pendás[a] and Tomás Rocha-Rinza*[b]

Received 22nd June 2016,
Accepted 7th July 2016

DOI: 10.1039/c6cp04386k

www.rsc.org/pccp

Resonance Assisted Hydrogen Bonds (RAHBs) are particularly strong H-Bonds (HBs) which are relevant in several fields of chemistry. The traditional explanation for the occurrence of these HBs is built on mesomeric structures evocative of electron delocalisation in the system. Nonetheless, there are several theoretical studies which have found no evidence of such electron delocalisation. We considered the origin of RAHBs by employing Quantum Chemical Topology tools, more specifically, the Quantum Theory of Atoms in Molecules (QTAIM) and the Interacting Quantum Atoms energy partition. Our results indicate that the π-conjugated bonds allow for a larger adjustment of electron density throughout the H-bonded system as compared with non-conjugated carbonyl molecules. This rearrangement of charge distribution is a response to the electric field due to the H atom involved in the hydrogen bonding of the considered compounds. As opposed to the usual description of RAHB interactions, these HBs lead to a larger electron localisation in the system, and concomitantly to larger QTAIM charges which in turn lead to stronger electrostatic, polarization and charge transfer components of the interaction. Overall, the results presented here offer a new perspective on the cause of strengthening of these important interactions.

1 Introduction

Hydrogen bonds (HBs) play a fundamental role in structural chemistry and biology.[1,2] Because of their mid-range strength and strong directionality, HBs are crucial in determining the structure and dynamics of a great diversity of molecular clusters and assemblies. For instance, the formation and dissociation of HBs at room temperature gives them an important role in many biochemical processes.[3]

Although a large amount of work has been developed to comprehend the essential features of H-bonds, many controversies still persist on this issue. For many authors the interaction is mainly electrostatic,[1,2,4,5] while others describe it as partially covalent.[6–12] Indeed, H-bonding is a very complex interaction which includes a wide variety of species and energy ranges: the formation energies of H-bonds cover the range from 0.2 to 40 kcal mol^{-1}.[13] Resonance assisted hydrogen bonds (RAHBs) are particularly strong HBs in uncharged molecules.[13,14] Since Gilli *et al.*[14–16] proposed the concept of RAHBs, this has had great success in many fields such as organic chemistry,[17–21] infrared spectroscopy,[22] nuclear magnetic resonance,[23] electron diffraction,[24] or biological chemistry.[25–28]

The proton donor and proton acceptor groups in RAHBs are connected through a chain of π-conjugated double bonds, and the standard explanation of the noticeable strength of these interactions is based on a chemically intuitive reasoning in which the conjugated bonds display an equalization of lengths through a pseudo-ring. This description of RAHBs is consistent with the deeply rooted idea that the existence of equivalent resonance structures is a stabilizing feature of a molecular system. As Fig. 1 shows, the tautomeric structures of malonaldehyde, an archetypal RAHB system, are evocative of a transfer of electron density in which the hydrogen bond acceptor turns into the hydrogen bond donor and *vice versa*.

Despite this chemically appealing explanation of RAHBs, many computational chemistry studies have failed so far to give indications of the presumed correlation between the amount of electron delocalisation and the energetics of these interactions. For example, the substitution of electron donating and withdrawing

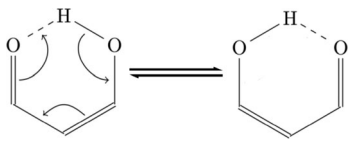

Fig. 1 Tautomeric structures related to the resonance assisted hydrogen bond in malonaldehyde.

[a] *Department of Analytical and Physical Chemistry, University of Oviedo, E-33006, Oviedo, Spain*
[b] *Institute of Chemistry, National Autonomous University of Mexico, Circuito Exterior, Ciudad Universitaria, Delegación Coyoacán C.P. 04510, Mexico City, Mexico. E-mail: tomasrocharinza@gmail.com*

† Electronic supplementary information (ESI) available. See DOI: 10.1039/c6cp04386k

groups in the system does not affect the energetics of different RAHBs.[29] Likewise, the analysis of the NMR properties of systems containing RAHBs developed by Alkorta and coworkers[30,31] showed that neither the proton chemical shifts nor the coupling constants point out to significant contributions from π-resonance to these interactions. On the contrary, it is put forward that the reason behind the RAHB strengthening lies in the σ-skeleton of the system.[32,33] Grabowski and coworkers used QTAIM analyses[34] to examine the nature of the stabilization in RAHBs. While they initially argued that the dissociation energy of intramolecular RAHBs depends mainly on the π-electron delocalisation,[35] they suggested in subsequent studies that the enhancement of electron delocalisation and the equalization of the length of the conjugated bonds do not correspond to the strengthening of the HBs.[36] In addition, ELF analyses have shown no difference between RAHBs and other intramolecular HBs found in molecules with saturated chains.[37] As a final example, valence bond theory has also been used to study the dimers of carboxylic acids, amides and malonaldehyde along with its substituted derivatives as model structures for intermolecular and intramolecular RAHBs.[38–40] Whereas most of the aforementioned investigations suggest that resonance stabilization energies are negligible as compared with the total interaction energies and that H-bond covalency is not significantly increased in RAHB interactions,[38,39] other studies propose that the delocalisation energy term is the main source of stabilisation in these HBs.[40]

With this background, the aim of this study is to contribute to the elucidation of the nature of RAHBs. For this purpose, we have considered a set of representative H-bonded molecules and clusters as shown in Fig. 2: (i) systems with intramolecular RAHBs (Fig. 2(a) and (b)), along with their non-conjugated counterparts (Fig. 2(c) and (d)), and (ii) the dimers of formic acid and formamide whose interactions have also been associated with intermolecular RAHB formation (Fig. 2(e) and (f)). We have used a battery of Quantum Chemical Topology (QCT) tools, more specifically the Quantum Theory of Atoms in Molecules (QTAIM)[34] and the Interacting Quantum Atoms (IQA) energy partition,[41,42] which together provide a good description of both long and short range interactions, a critical issue in this research. The QTAIM and IQA wavefunction analyses (i) are based on orbital invariant quantities, namely, the reduced first order density matrix $\varrho_1(\mathbf{r}_1,\mathbf{r}_1')$ along with the pair density $\varrho_2(\mathbf{r}_1,\mathbf{r}_2)$ and (ii) provide a division of the electronic energy in components endowed with a well-defined physical meaning. In this sense, they offer answers which do not depend on the specific method used to perform the underlying calculations. Their conclusions are thus free of method biases. Most importantly, IQA and QTAIM have already been used successfully to analyze the nature of the hydrogen bond[5] and to study H-bond cooperative[43] and anticooperative[44] effects in water clusters. In this sense, they open a unique reference-free window to understand the reasons behind the strengthening or weakening of HBs. Altogether, these wavefunction analyses enable us to provide an orbital invariant view of the origin of the strength of RAHBs, in which resonance and electrostatic effects are naturally separated. We propose that electrostatics, polarization and charge transfer play a crucial role within RAHBs on account of a redistribution of the electron density which leads to an overall decrease in electron delocalisation throughout the system. These effects are boosted by the conjugated π system. We offer in this way a new perspective on the origin of the important RAHB interactions.

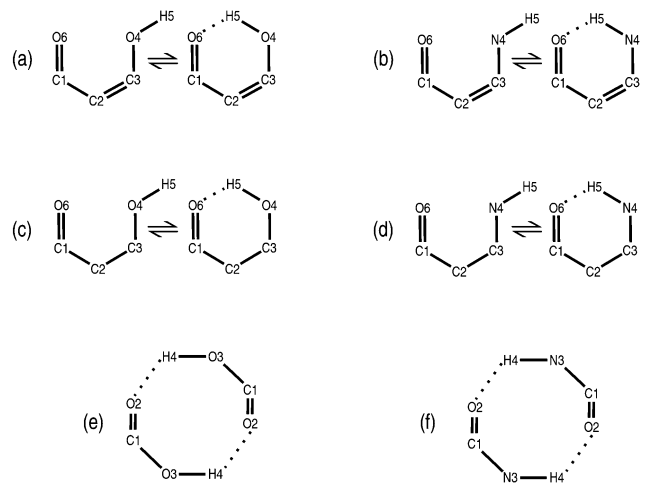

Fig. 2 Structure of the systems studied in the present work. The valency of every atom is complete, we are addressing closed shell systems in every case but some hydrogens have been omitted for the sake of clarity.

2 Methods

The quantum theory of atoms in molecules is based on a topological analysis of the electron density, $\varrho(\mathbf{r})$, which conduces to a partition of the three-dimensional space in disjoint regions (Ω) identified with the atoms of chemistry.[34] The QTAIM basins constitute appropriate subsystems for which one can compute the average values of quantum-mechanical observables, that is to say, atomic properties usually denoted as $\langle A\rangle_\Omega$.[45] The addition of the quantities $\langle A\rangle_\Omega$ across a complete molecule or molecular cluster equals the expectation value of the corresponding operator for the whole system. As stated in the Introduction of this paper, different types of chemical bonds such as covalent and intermolecular interactions can be characterized by means of QTAIM on the same rigorous basis. With this intention in mind, we determined the charges associated with each QTAIM atom, and carried out the integration of the Fermi and Coulomb holes[46] over one or two different basins to determine the localisation (LI) and delocalisation (DI) indices[34] used to analyse the change in the number of delocalised electrons across the system due to the formation of every considered HB.

In addition, we used the QTAIM division as a starting point to perform the partition of the Born–Oppenheimer electronic energy, E, in accordance with the IQA approach[41,42]

$$E = \sum_{\mathrm{A}} E^{\mathrm{A}}_{\mathrm{net}} + \frac{1}{2}\sum_{\mathrm{A}}\sum_{\mathrm{B}\neq\mathrm{A}} E^{\mathrm{AB}}_{\mathrm{int}}, \qquad (1)$$

in which E^{A}_{net} represents the net energy of basin A and E^{AB}_{int} denotes the interaction energy between atoms A and B. In addition, E^{A}_{net} and E^{AB}_{int} can be further split into

$$E^{A}_{net} = T^{A} + V^{AA}_{ne} + V^{AA}_{ne}, \quad (2)$$

$$E^{AB}_{int} = V^{AB}_{nn} + V^{AB}_{ee} + V^{AB}_{ne} + V^{BA}_{ne}, \quad (3)$$

wherein T^{A} is the kinetic energy of atom A, whilst $V^{XY}_{\nu\mu}$ indicates the potential energy due to the interaction of ν in atom X with μ in atom Y, with the labels ν and μ representing either electrons or nuclei. The detailed expressions of every term in the RHS of eqn (2) and (3) as functionals of the first-order reduced density matrix, $\varrho_1(\mathbf{r}_1,\mathbf{r}_1')$, or the pair density, $\varrho_2(\mathbf{r}_1,\mathbf{r}_2)$ are given in ref. 41 and 42.

The interaction between two atoms can be further characterized by considering the Coulombic (J) and exchange–correlation (xc) components of the pair density

$$\varrho_2(\mathbf{r}_1,\mathbf{r}_2) = \varrho^{J}_2(\mathbf{r}_1,\mathbf{r}_2) + \varrho^{xc}_2(\mathbf{r}_1,\mathbf{r}_2), \quad (4)$$

which leads to a similar separation of the electron–electron part of E^{AB}_{int},

$$V^{AB}_{ee} = V^{AB}_{J} + V^{AB}_{xc}. \quad (5)$$

This results in a division of the IQA interaction energy in a classical, that is, electrostatic,

$$V^{AB}_{cl} = V^{AB}_{J} + V^{AB}_{ne} + V^{BA}_{ne} + V^{AB}_{nn}, \quad (6)$$

and a quantum, *i.e.*, exchange–correlation part, so that

$$E^{AB}_{int} = V^{AB}_{cl} + V^{AB}_{xc}. \quad (7)$$

Since the Hartree–Fock (HF) method considers only Fermi correlation, V^{AB}_{xc} becomes V^{AB}_{x} when we consider density functions derived from this approximation.

3 Computational details

The geometry of every system was optimized using the MP2[47] approximation in its efficient RIJCOSX variant[48] along with the aug-cc-pVTZ basis set,[49] as implemented in the Orca program.[50] It has been reported that O–H···O hydrogen-bonded systems are properly described by second-order Møller–Plesset perturbation theory together with augmented Dunning basis sets.[51] In order to analyse the changes in a system when an HB is formed or dissociated, we normally compare the properties of the interacting monomers (i) within the molecular cluster in question and (ii) when the fragments linked by an H-bond are taken apart from each other. Such a procedure is straightforward for dimers (e) and (f). It is not, however, for the rest of the systems (a)–(d) wherein the RAHBs under examination are intramolecular. Hence, we contrasted the properties of these molecules in the non-hydrogen-bonded structure and the conformation in which the HB is formed, so as to determine the formation energy of each RAHB as shown in the left and right parts respectively of Fig. 2(a)–(d).

We performed afterwards the IQA and QTAIM wavefunction analyses based on HF density functions. The HF wavefunctions were computed using the Gamess-US[52] program. The IQA partition based on $\varrho^{HF}_1(\mathbf{r}_1,\mathbf{r}_1')$ and $\varrho^{HF}_2(\mathbf{r}_1,\mathbf{r}_2)$ has been successfully used recently to study the H-bond cooperative effects within small water clusters.[43] Besides, the RAHB formation energies examined in this work are considerably larger in magnitude than those associated with these H_2O systems[43,53] and hence easier to study from an energetic perspective. Finally, the behaviour of the HF and MP2 electron densities, as reflected in the changes in delocalisation indices upon the formation of the HB, is very similar. The corresponding data are summarized in Table S1 in the ESI.†

The IQA partition energy and the QTAIM analyses were performed using the Aimall[54] package. Finally, we used the programs Avogadro[55,56] and Gnuplot[57] for molecular and data visualization respectively.

4 Results and discussion

A deeply rooted chemical conception establishes that resonance is a stabilizing effect. However, uncovering the physical nature of that purported stabilization is far from trivial, as the severe problems encountered when trying to define resonance (*e.g.* aromatic) stabilization energies have taught us over the years.[58] As we show below, uncoupling the several effects that charge delocalisation channels open up may lead to several unexpected results. Fortunately, these effects are easy to isolate using a reference-free real space energy decomposition method like IQA.

As established in previous studies on H-bonds,[13,43,44,59,60] the formation of an RAHB leads to a noticeable redistribution of electron density across the molecule. These changes are in agreement with conventional arrow pushing in conjugated unsaturated systems. This electron pushing is suggestive of bond length equality throughout the molecule. The experimentally accessible tendency of equalization of bond distances in these compounds can be analyzed by means of electron sharing descriptors. Since delocalisation indices are direct sharing indicators, we first consider the differences in the DI values in (i) the open non-hydrogen-bonded conformations of systems (a)–(d), *i.e.*, those having their H-bond dissociated, which are shown in the left part of Fig. 2(a)–(d), and (ii) the corresponding closed configurations, namely, those resulting from the formation of the H-bond as displayed in right of Fig. 2(a)–(d).

Fig. 3 shows how the DIs of the conjugated bonds change on the formation of the HB for systems (a) and (b).‡ In agreement with chemical intuition, the opening of the π conjugating channel that accompanies the formation of the H-bond induces a rather large scale reorganization of the pair density with the DIs nicely reflecting the resonance structures in Fig. 1. This effect is mostly absent in non-conjugated systems, and the

‡ The use of MP2 density functions and the Müller approximation to the second-order density yields changes in the delocalisation indices which are very similar than those obtained by means of HF wavefunctions. Both sets are presented in Table S1 in the ESI.†

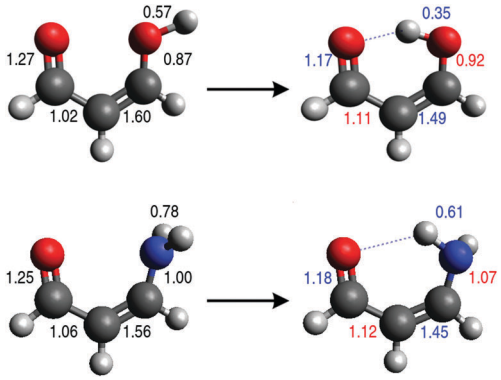

Fig. 3 Delocalisation indices of compounds (a) and (b) in the non-H-bonded conformation (left) and the structure in which the resonance assisted hydrogen bond is formed (right). We present in red the values of δ(A,B) that increase with the formation of the H-bond, whereas those diminished in the same process are reported in blue.

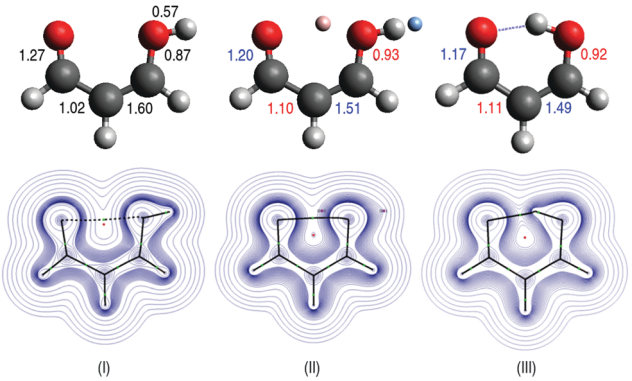

Fig. 4 Top, delocalisation indices in different conformations of compound (a). On the left (right) is the open (closed) conformation. At the center is the open conformation with a positive point charge q = 0.6e, indicated in pink, added to the non-H-bonded conformation. A negative charge of the same magnitude was also included (light blue) to keep the system electrically neutral. We present in red the values of δ(A,B) that increase with respect to those in the open configuration in the absence of the point charges, while those that are diminished with respect to the same reference are reported in blue. Bottom- density contours of the aforementioned systems.

Table 1 Changes in the QTAIM charges of different atoms upon the formation of the HB and its sum of absolute values. Atomic units are used throughout

Atom	(a)	(b)	(c)	(d)
C1	−0.130	−0.080	−0.018	−0.008
C2	−0.047	−0.033	0.000	−0.016
C3	0.144	0.107	0.025	0.015
O4/N4	−0.084	−0.092	−0.026	−0.006
H5	0.092	0.124	0.040	0.032
O6	−0.050	−0.036	−0.012	−0.004
Sum	0.546	0.473	0.122	0.080

corresponding changes in systems (c) and (d) are very small. More quantitatively, the values of δ(O4,H5) and δ(N4,H6),§ *i.e.* the DIs associated with the covalent bonds O–H and N–H in compounds (a) and (b), respectively, are reduced with the formation of the RAHB, the decrease of the former being larger than that of the latter. In addition, the double bonds involving one or two carbon atoms reduce their number of shared electrons, whereas the single bonds increase their associated DIs. In this way, a number of delocalised electrons become more evenly distributed across the conjugated π systems.

Since $\varrho(\mathbf{r})$ may be obtained by tracing out one electron coordinate from $\varrho_2(\mathbf{r}_1,\mathbf{r}_2)$, it is not surprising that the changes in the latter scalar field will also be evidenced through the analysis of the charge distribution. Table 1 shows the variation in the most relevant QTAIM atomic charges, ΔQ, after H-bond formation. We can clearly sort the systems into conjugated/non-conjugated ones, and within each of these classes into O–H/N–H containing molecules. We note that (i) the formation of the H-bond induces a charge redistribution that increases the overall total atomic charge (in absolute value), this effect being considerably larger in conjugated systems; and (ii) the changes in atomic charges are slightly larger than those we have found in small water clusters with σ H-bond cooperative effects.[43] In chemically appealing terms, the π channel allows for a more efficient charge density flow.

§ The labels of the atoms are shown in Fig. 2.

We can now examine the origin of the one-electron and pair density reorganization. The IQA approach has been used to show that the charge distribution changes in H-bonded dimers containing only σ-bonds result mostly from the self-consistent classical polarization induced by the interacting monomers on each other.[5] To examine a similar possibility herein, we simulated the electrostatic effect of the change in the position of the hydrogen donor group accompanying H-bond formation by placing two point charges on the open conformation of (a) with $q = \pm 0.6e$.¶ The positive charge is located at the position of the bridging H atom in the closed conformer, and the cancelling negative one in close proximity‖ to the enolic hydrogen atom of (a).

As the central panels of Fig. 4 show, the model reproduce very well the DIs of the RAH-bonded compound. Once again, the change in the electric field experienced by the system upon H-bond formation is the basic factor determining charge reorganization. Furthermore, these changes explain the pair density variations. This is an important new insight that admits the following interpretation: π channels are more efficient roads to charge flow than σ ones, as expected, but aromatic-like resonance is not needed to understand bond-order equalization and charge transfer in these systems. They come out as the response of the mobile π electrons to the new electric field.

Thus, the role of resonance itself in the stabilization of RAHB systems should be questioned. Further evidence on this issue is easily found. A remarkably simple argument comes from the total number of delocalised electrons in the system: if resonance is a basic energetic factor in RAHBs, the formation of

¶ This value corresponds to the QTAIM charge of the bridging hydrogen within compound (a) when the RAHB is formed.

‖ The shortest distance between the negative point charge and the nucleus of the bonding H atom in the upper part of Fig. 4(II) that allowed us to perform a successful electronic structure calculation was 0.1 Å.

these H-bonds should result in an increase of this quantity. As we show now, the condition that the delocalisation indices are more uniformly distributed among the system does not imply that their total sum is increased. By considering the division of electrons using LIs and DIs,

$$N = \sum_{A} \lambda(A) + \frac{1}{2}\sum_{A\neq B} \delta(A,B) \quad (8)$$

we note that the total number of delocalised $\left(\frac{1}{2}\sum_{A\neq B}\delta(A,B)\right)$ electrons decreases (Table 2) after the formation of the H-bond. Such a reduction is of course accompanied by a concomitant increase in the total number of localised electrons, and becomes a powerful argument against the traditional role assigned to resonance in RAHBs, in agreement with previous experimental and theoretical studies which found no indication of an increased electron delocalisation in these types of H-bonds.[29–33,36–40]

Since, as stated above, the interacting quantum atom partition provides a unique combination of electron and energy descriptors, we may now explore the energy features of the formation of the HB associated with the previously discussed changes in $\varrho(\mathbf{r})$ and $\varrho_2(\mathbf{r}_1,\mathbf{r}_2)$. Following the previous line of reasoning, we first examine the energetics of resonance and bond order equalization, which are indicated in terms of the covalent, *i.e.* exchange, IQA contributions. Table 2 reports the variation in the intra-atomic and interatomic exchange contributions which result from the formation of the H-bond for systems (a)–(d). In agreement with our previous discussion, the overall interatomic covalent stabilization decreases in magnitude, at the expense of an increase of the absolute value of the intra-atomic counterpart. Again, all the atomic and interatomic changes reported in Table 2 are considerably larger in the conjugated systems, giving further support to the notion that resonance is not the direct cause of the strengthening of RAHBs.

Table 2 Changes in the sum of (i) delocalisation indices (δ^{AB}), (ii) the intra-atomic (V_x^A) and (iii) interatomic (V_x^{AB}) exchange components of the electronic energy upon the formation of the corresponding hydrogen bonds. Energy values in kcal mol^{-1}

System	$\frac{1}{2}\sum_{A\neq B}\Delta\delta^{AB}$	$\sum_{A}\Delta V_x^A$	$\frac{1}{2}\sum_{A\neq B}\Delta V_x^{AB}$
(a)	−0.10	−31.77	16.81
(b)	−0.07	−23.71	17.00
(c)	−0.03	−10.37	6.62
(d)	−0.01	−3.19	2.07

Besides the energy partition into intra and interatomic contributions just presented, it is also relevant to study the local IQA contributions within the six-membered pseudo-rings in Fig. 2. We discuss first the bonding energetics between the atoms directly involved in the HB interaction, *i.e.*, O···H–X where X = O for (a), (c) and X = N in (b), (d) as reported in Table 3. In order to consider suitable references for discussion purposes, we also present the results for the $(H_2O)_2$ and $H_2O\cdots H_3N$ clusters, with no σ or π cooperative effects whatsoever. We point out that classical interaction energies V_{cl}^{AB} include all the electrostatic, polarization and charge transfer contributions to the interaction that are usually considered in perturbation-like approaches, as suggested in ref. 43.

Because all the interactions occur between considerably charged atoms, the classical component dominates over the exchange–correlation in every entry of Table 3 as expected, representing more than 90% of E_{int}^{AB} in the O···H and O···X cases. It also represents more than 65% in all instances of the O–H bonds, comprising a smaller percentage for the N–H bonds in molecules (b) and (d). As a matter of fact, there is a good correlation between the magnitudes of V_{cl}^{AB} and those obtained from a naïve Coulomb law approach, that is, considering only the IQA monopole–monopole energy. Due to smaller charge polarization, the values of $V_{cl}^{O\cdots H}$ are 35% smaller for the saturated systems as revealed by comparing systems (a)–(c) and (b)–(d).

Regarding V_x^{AB} the O···H component correlates with the strength of the H-bond, in correspondence with previous studies.[5,43] This reveals that the conjugated systems display stronger interactions than their saturated analogues, in which the H-bonds are even weaker than those between $H_2O\cdots H_2O$ and $H_2O\cdots H_3N$. We stress however, that the local enhancement of $E_{int}^{O\cdots H}$ in (a) and (b) is obviously dominated by the classical, not the exchange terms. In this way, IQA unveils that the increased strength of the local H-bond interaction in the RAHB moieties, despite including both exchange and classical contributions, is dominated by the latter component. Moreover, although $V_X^{O\cdots H}$ is larger in system (a) than it is, for example, in $H_2O\cdots H_2O$ and $H_2O\cdots H_3N$, the overall reduction of the magnitude of $\frac{1}{2}\sum_{A\neq B}V_x^{AB}$ shown in Table 2 means that the strengthening of the H-bond by means of electron sharing is accompanied by the weakening of other covalent interactions in the system. IQA provides no indication that the O···H–X system is stabilized by means of π-resonance effects.[13,14]

To gain further insight, we now consider the role played by the rest of the atoms apart from the O···H–X moiety in the

Table 3 IQA interaction energies along with their classical and exchange parts, for the O···H, O···X, and X–H bonds, directly involved in the intramolecular non-covalent interactions under examination. X represents O in compounds (a), (b) and N in systems (c), (d). The data for the water dimer are also presented for comparison. The data are reported in kcal mol^{-1}

System	$E_{int}^{O\cdots H}$	$V_{cl}^{O\cdots H}$	$V_x^{O\cdots H}$	$E_{int}^{O\cdots X}$	$V_{cl}^{O\cdots X}$	$V_x^{O\cdots X}$	E_{int}^{X-H}	V_{cl}^{X-H}	V_x^{X-H}
(a)	−208.54	−193.45	−15.10	243.41	257.14	−13.73	−416.49	−345.07	−71.42
(b)	−134.35	−125.12	−3.58	238.08	247.40	−9.33	−354.60	−231.34	−123.26
(c)	−129.05	−125.47	−9.23	204.33	209.48	−5.15	−386.68	−279.74	−106.94
(d)	−71.22	−68.13	−3.08	163.75	166.72	−2.97	−274.04	−115.16	−158.88
$H_2O\cdots H_2O$	−141.04	−133.38	−7.66	182.60	187.91	−5.31	−387.79	−289.18	−98.61
$H_2O\cdots H_3N$	−76.96	−71.74	−5.21	146.82	150.62	−3.79	−268.33	−113.25	−155.08

formation of the RAHBs under examination. Indeed, the IQA components involving the atoms that do not participate directly in the HB have to be accounted into the energetics of these interactions as well.[43] For instance, $(H_2O)_2$ presents a smaller magnitude of $\left|V_{cl}^{H_2O\cdots H_2O}\right|$ with respect to $\left|V_{x}^{H_2O\cdots H_2O}\right|$ due to the cancellation of the attractive O···H interactions with the repulsive O···O and H···H contacts as explained in the discussion of Fig. 10 in ref. 43. This is a relatively common result: the strong electrostatic interactions tend to cancel out within neutral systems. These analyses are obscured in the case of intramolecular H-bonds, for there is no natural partition of the atoms of the molecule into interacting fragments. Nonetheless, we can use the dimers of formic acid and formamide, adducts (e) and (f), to make a comparison with $(H_2O)_2$ and $H_2O\cdots H_3N$ clusters on similar grounds. Table 4 shows that neither HCOOH···OC(H)OH nor $HCONH_2\cdots$OC(H)NH2 shows larger exchange to interaction energy ratios than their corresponding non-resonance assisted dimers, thereby supporting our previous conclusions.

Table 4 IQA interaction energies together with their classical and exchange components between the monomers in the HCO_2H, $HCONH_2$ and H_2O dimers (on a per H-bond basis) as well as the total deformation energy per molecule. The values are given in kcal mol^{-1}

System	E_{int}^{AB}	V_{cl}^{AB}	V_{x}^{AB}	E_{def}^{A}
Formic acid (e)	−41.61	−16.52	−25.09	33.64
Formamide (f)	−32.17	−12.99	−19.17	26.21
Water	−19.86	−6.68	−13.17	8.17

One of the capabilities of IQA and QTAIM wavefunction analyses is to offer views at different levels of granularity, hence it is also interesting to discuss some of the specific interatomic interactions, particularly those along the pseudo-rings in Fig. 2(a)–(d). As Fig. 5 shows, H-bond formation has a strong influence on all the bonds forming the framework of the six-membered ring. It is clear that electrostatics dominates most of the interactions, for in all cases the change in E_{int}^{A-B} has the same sign as that of V_{cl}^{A-B} and in the majority of instances (the $C^{\alpha}{=}C^{\beta}$ bonds in malondialdehyde and β-amine acrolein being notable exceptions) ΔV_{cl}^{A-B} is the major contribution to ΔE_{int}^{A-B}, that is, $\Delta V_{cl}^{A-B}/\Delta E_{int}^{A-B} > 0.5$.

The aforementioned preponderance of the IQA classical component is in agreement with a previous analysis of resonance assisted hydrogen bonded adenine–thymine pairs and other analogue compounds[61] where no changes in relative stability were found when the aromatic rings were removed. The corresponding EDA analysis[62] shows that the stronger HBs in the unsaturated systems originates from larger electrostatic interactions. Separately, Mo and coworkers, using real space techniques, arrived at similar conclusions.[63] Altogether, our results indicate that an RAHB involves a considerable rearrangement of both the one- and two-particle densities facilitated by the π-conjugated system, which leads to an overall electron localisation and a large separation of charges. It is through the latter, which would be interpreted as a combination of charge transfer and polarization effects, that the RAHB systems acquire their particular stability.

The alternating pattern of V_{x}^{A-B} in the diagrams of Fig. 5 is reminiscent of the equalization of DIs previously discussed as a

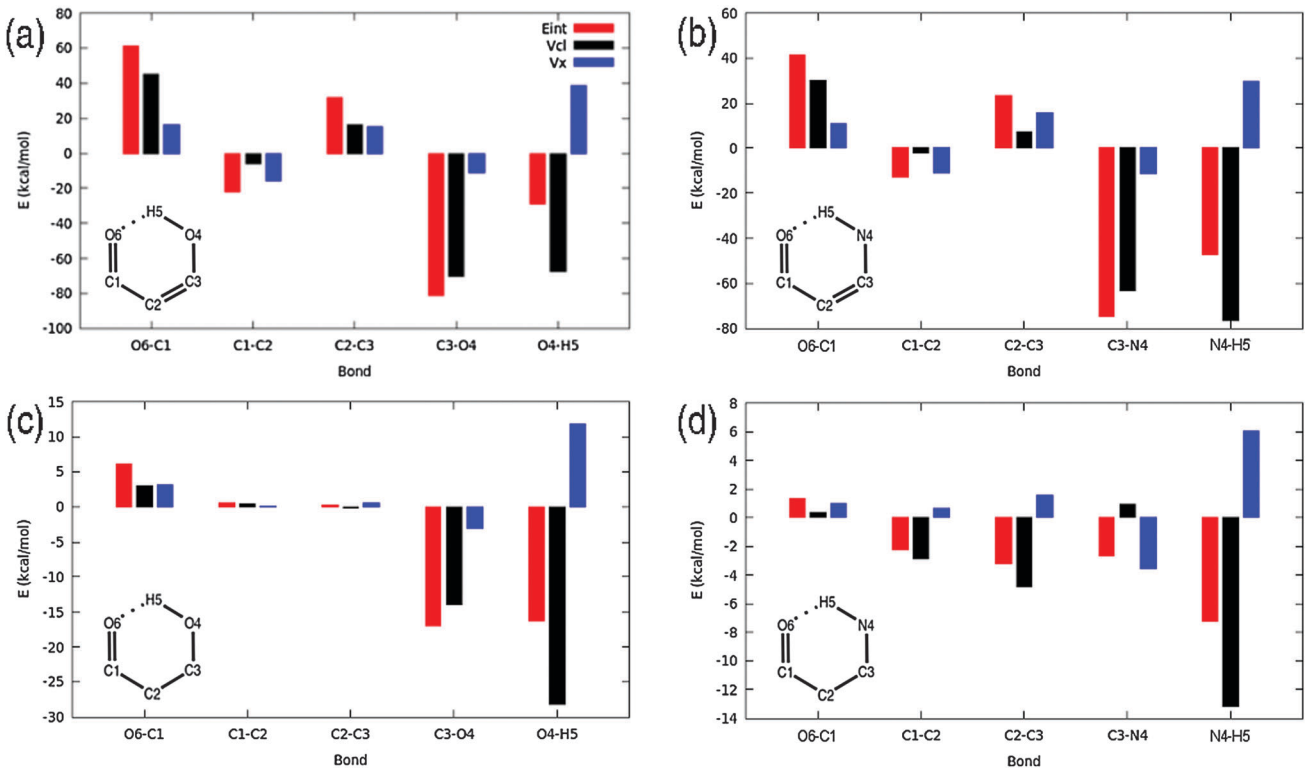

Fig. 5 Changes in IQA interaction components accompanying the formation of H-bonds in systems (a)–(d). Note the different scales used in the graphs.

distinctive feature of the stabilization mediated by conjugation in RAHBs. A major insight results from the observation that such alternation is mostly absent in the saturated systems (c) and (d). As expected, covalent conjugation effects are not found in the saturated molecules. In all cases the formation of the H-bond makes the corresponding X–H bond less covalent ($\Delta V_{x}^{X-H} > 0$) and more ionic ($\Delta V_{cl}^{X-H} < 0$), a fact that supports the superior contribution of electrostatics over covalency in these systems. Similar insights can be obtained for the rest of the ring bonds. Finally, we emphasize that the changes in all the energetic components are overall larger in magnitude for the conjugated compounds, in line with the larger charge density flow allowed by the π channels.

5 Conclusions

We have considered the origin of the RAHB interaction by means of quantum chemical topology. Our results indicate that the electric field due to the bridging hydrogen induces a strong redistribution of the electron density in the conjugated molecules CHO–CH═CH–OH and CHO–CH═CH–NH_2, which leads to a decrease in the electron delocalisation within the system as opposed to the usual explanation of the resonance assisted H-bonds. Indeed, the intra-atomic exchange contribution of the electron energy increases at the expense of the corresponding interatomic counterpart. The IQA and QTAIM analyses indicate that the π channels of the analyzed conjugated carbonyls allow for a greater reorganization of the one and two-electron distributions which lead to important contributions from electrostatics, polarization and charge transfer in the establishment of an RAHB. On the whole, we anticipate that the new interpretation of the resonance assisted hydrogen bonds presented herein will prove valuable in the understanding of these important interactions in different fields of physical chemistry.

Acknowledgements

The authors acknowledge financial support from DGAPA/UNAM (project PAPIIT IN209715) and the Spanish government (grant CTQ-2015-65790-P) as well as computer time from DGTIC/UNAM (grant SC16-1-IG-99). T. R.-R., E. R. M. and J. M. G. V. are also grateful to CONACyT/México for financial support (grant 253776), MSc and PhD scholarships (number 308773 and 381483) respectively. T. R.-R. is also thankful to Magdalena Aguilar Araiza, Gladys Cortés Romero and David Vazquez Cuevas for technical support.

References

1 G. R. Desiraju and T. Steiner, *The Weak Hydrogen Bond*, Oxford University Press, New York, 1999.
2 G. A. Jeffrey, *An introduction to Hydrogen Bonding*, Oxford University Press, New York, 1997.
3 G. Gilli and P. Gilli, *THEOCHEM*, 2000, **1**, 552.
4 L. Pauling, *The nature of Chemical Bond*, Cornell University Press, New York, 1960.
5 Á. Martn Pendás, M. A. Blanco and E. Francisco, *J. Chem. Phys.*, 2006, **125**, 184112.
6 A. R. Reed, L. A. Curtiss and F. Weinhold, *Chem. Rev.*, 1988, **88**, 899.
7 W. H. Thompson and J. T. hynes, *J. Am. Chem. Soc.*, 2000, **122**, 6278.
8 E. D. Isaacs, A. Shukla, P. M. Platzman, D. R. Hamann, B. Barbiellini and C. A. Tulk, *Phys. Rev. Lett.*, 1999, **82**, 600.
9 K. G. Tapan, N. S. Viktor, R. K. Patrick and R. D. Ernest, *J. Am. Chem. Soc.*, 2000, **122**, 1200.
10 A. H. Pakiari and K. J. Eskandari, *THEOCHEM*, 2006, **51**, 759.
11 S. J. Grabowski, J. Sokalski and W. A. Leszczynki, *J. Phys. Chem. A*, 2005, **109**, 4331.
12 S. J. Grabowski, *Chem. Rev.*, 2011, **111**, 2597.
13 T. Steiner, *Angew. Chem., Int. Ed.*, 2002, **41**, 48.
14 G. Gilli, F. Bellucci, V. Ferretti and V. Bertolasi, *J. Am. Chem. Soc.*, 1989, **111**, 1023.
15 V. Bertolasi, P. Gilli, V. Ferretti and G. Gilli, *J. Am. Chem. Soc.*, 1991, **8**, 4917.
16 P. Gilli, V. Bertolasi, V. Ferretti and G. Gilli, *J. Am. Chem. Soc.*, 1994, **116**, 909.
17 J. Chin, C. K. Dong, H. J. Kim, F. B. Panosyan and M. K. Kwan, *Org. Lett.*, 2004, **6**, 2591.
18 H. Kim, Y. Nguyen, C. P. H. Yen, L. Chagal, A. J. Lough, B. M. Kim and J. Chin, *J. Am. Chem. Soc.*, 2008, **130**, 12184.
19 M. Palusiak, S. Simon and M. Solà, *J. Org. Chem.*, 2006, **71**, 5241.
20 M. Palusiak, S. Simon and M. Solà, *J. Org. Chem.*, 2009, **74**, 2059.
21 T. M. Krygowski, J. E. Zachara-Horeglad and M. Palusiak, *J. Org. Chem.*, 2010, **75**, 4944.
22 M. Rospenk, P. Majewska, B. Czarnik-Matusewicz and L. Sobczyk, *Chem. Phys.*, 2006, **326**, 458.
23 R. Marković, A. Shirazi, Z. Džambaski, M. Baranac and D. Minić, *J. Phys. Org. Chem.*, 2004, **17**, 118.
24 R. Srinivasan, J. S. Feenstra, S. T. Park, S. Xu and A. H. Zewail, *J. Am. Chem. Soc.*, 2004, **126**, 2266.
25 J. Emsley, *Struct. Bonding*, 1984, **57**, 147.
26 P. S. Corbin and S. C. Zimmerman, *J. Am. Chem. Soc.*, 1998, **120**, 9710.
27 C. Fonseca-Guerra, F. M. Bickelhaupt, J. G. Snijders and E. J. Baerends, *Chem. – Eur. J.*, 1999, **5**, 3581.
28 J. Sponer, P. Jurecka and P. Hobza, *J. Am. Chem. Soc.*, 2004, **126**, 10142.
29 L. González, O. Mó and M. Yáñez, *J. Org. Chem.*, 1999, **64**, 2314.
30 I. Alkorta, J. Elguero, O. Mó, M. Yáñez and J. E. Del Bene, *Mol. Phys.*, 2004, **102**, 2563.
31 I. Alkorta, J. Elguero, O. Mó, M. Yáñez and J. E. Del Bene, *Chem. Phys. Lett.*, 2005, **411**, 411.
32 P. Sanz, O. Mó, M. Yañez and J. Elguero, *J. Phys. Chem. A*, 2007, **111**, 3585.
33 T. M. Krygowski and J. E. Zachara-horeglad, *Tetrahedron*, 2010, **65**, 2010.

34 R. F. W. Bader, *Atoms in molecules: A Quantum Theory*, Oxford University Press, 1990.
35 S. J. Grabowski, *J. Phys. Org. Chem.*, 2003, **16**, 797.
36 R. W. Gora, S. J. Grabowski and J. Leszczynski, *J. Phys. Chem. A*, 2005, **109**, 6397.
37 F. Fuster and S. J. Grabowski, *J. Phys. Chem. A*, 2011, **115**, 10078.
38 J. F. Beck and Y. Mo, *J. Comput. Chem.*, 2006, **28**, 455.
39 Y. Mo, P. Bao and J. Gao, *Phys. Chem. Chem. Phys.*, 2011, **13**, 6760.
40 R. W. Gora, M. Maj and S. J. Grabowski, *Phys. Chem. Chem. Phys.*, 2013, **15**, 2514.
41 M. A. Blanco, Á. Martn Pendás and E. Francisco, *J. Chem. Theory Comput.*, 2005, **1**, 1096.
42 E. Francisco, Á. Martín Pendás and M. Blanco, *J. Chem. Theory Comput.*, 2006, **2**, 90.
43 J. M. Guevara-Vela, R. Chávez-Calvillo, M. García-Revilla, J. Hernández-Trujillo, O. Christiansen, E. Francisco, A. Martín Pendás and T. Rocha-Rinza, *Chem. – Eur. J.*, 2013, **19**, 14304.
44 J. M. Guevara-Vela, E. Romero-Montalvo, V. A. Mora-Gómez, R. Chávez-Calvillo, M. García-Revilla, E. Francisco, Á. Martín Pendás and T. Rocha-Rinza, *Phys. Chem. Chem. Phys.*, 2016, DOI: 10.1039/C6CP00763E.
45 R. F. W. Bader, *Chem. Rev.*, 1991, **91**, 893.
46 X. Fradera, M. A. Austen and R. F. W. Bader, *J. Phys. Chem. A*, 1999, **103**, 304.
47 C. Møller and M. S. Plesset, *Phys. Rev.*, 1934, **46**, 618.
48 S. Kossmann and F. Neese, *J. Chem. Theory Comput.*, 2010, **6**, 2325.
49 T. H. Dunning, *J. Chem. Phys.*, 1989, **90**, 1007.
50 F. Neese, *Wiley Interdiscip. Rev.: Comput. Mol. Sci.*, 2012, **2**, 73.
51 C. Pérez, M. T. Muckle, D. P. Zaleski, N. A. Seifert, B. Temelso, G. C. Shields, Z. Kisiel and B. H. Pate, *Science*, 2012, **336**, 897.
52 M. W. Schmidt, K. K. Baldridge, J. A. Boatz, S. T. Elbert, M. S. Gordon, J. J. Jensen, S. Koseki, N. Matsunaga, K. A. Nguyen, S. Su, T. L. Windus, M. Dupuis and J. A. Montgomery, *J. Comput. Chem.*, 1993, **14**, 1347.
53 G. Gilli, V. Bertolasi, V. Ferretti and P. Gilli, *Acta Crystallogr., Sect. B: Struct. Sci.*, 1993, **49**, 564.
54 T. A. Keith, *Aimall, version 16.01.09*, tk gristmill software, 2012, aim.tkgristmill.com.
55 Avogadro: an open-source molecular builder and visualization tool. Version 1.XX. http://avogadro.openmolecules.net/.
56 M. D. Hanwell, D. E. Curtis, D. C. Lonie, T. Vandermeersch, E. Zurek and G. R. Hutchison, *J. Cheminf.*, 2012, **4**, 17.
57 http://gnuplot.sourceforge.net/.
58 A. Stanger, *Chem. Commun.*, 2009, 1939.
59 L. Albrecht and R. J. Boyd, *J. Phys. Chem. A*, 2012, **116**, 3946.
60 L. Albrecht, R. J. Boyd, O. Mó and M. Yáñez, *Phys. Chem. Chem. Phys.*, 2012, **14**, 14540.
61 L. Guillaumes, S. Simon and C. FonsecaGuerra, *ChemistryOpen*, 2015, **4**, 318.
62 E. D. Glendening and A. Streitwieser, *J. Chem. Phys.*, 1994, **100**, 2900.
63 Y. Mo, *J. Mol. Model.*, 2006, **12**, 665.

